Supporting Information

Thermal Modulation of Surface-Enhanced Raman Scattering and Plasmon-induced Catalysis in Ag Nanoparticle/ZnO Microrod Composites

Yinong Wang[a], Rui Liu[a], Zhiyue Zhong[a], Jinpeng Liu[a], Xiao Feng[b], Lizhao Liu[a*], Feng Jiang[a*]

[a]Dalian University of Technology, Dalian 116024, Liaoning, China.

[b]University of Leicester, Leicester LE1 7RH, U.K.

E-mail: lizhao_liu@dlut.edu.cn; jiangfeng@dlut.edu.cn.

1. Material and methods

In the experiment, 0.01 mol $Zn(CH_3COO)_2 \cdot 2H_2O$ was added to 40 mL water with stirring for 60 minutes to give a uniform solution. This solution was subsequently transferred into a Teflon-lined stainless-steel autoclave with a capacity of 50 mL. The autoclave was then sealed and maintained at 150 ˚C for 24 h. Hexagonal ZnO microrods were obtained after washing with deionized water and drying under N_2. Ag NPs were deposited onto these microrods via a vacuum sputtering procedure with a duration of 2 s using a QUORUM Q150TES system. The resulting samples were characterized using X-ray diffraction (XRD, Shimadzu XRD-7000S) with Cu $K_\alpha 1$ radiation (λ=1.5406 Å). The morphologies of the samples were studied using scanning electron microscopy (SEM, FEI Nova NanoSEM 450) and transmission electron microscopy (TEM, FEI Tecnai-G2F30). Energy-dispersive X-ray spectroscopy (EDS) data were also acquired with the SEM instrument. During the SERS analysis, R6G molecules were adsorbed from an ethanol solution onto Ag NPs deposited on hexagonal ZnO microrods, after which the material was washed with pure ethanol to remove any excess R6G molecules. SERS spectra were collected using a confocal micro-Raman spectrometer (Renishaw inVia) through a 50× objective lens. A laser beam with wavelength of 532 nm, spot size of approximately 1.5 μm^2, and intensity of approximately 100 μW was employed.

2. Structural characterization

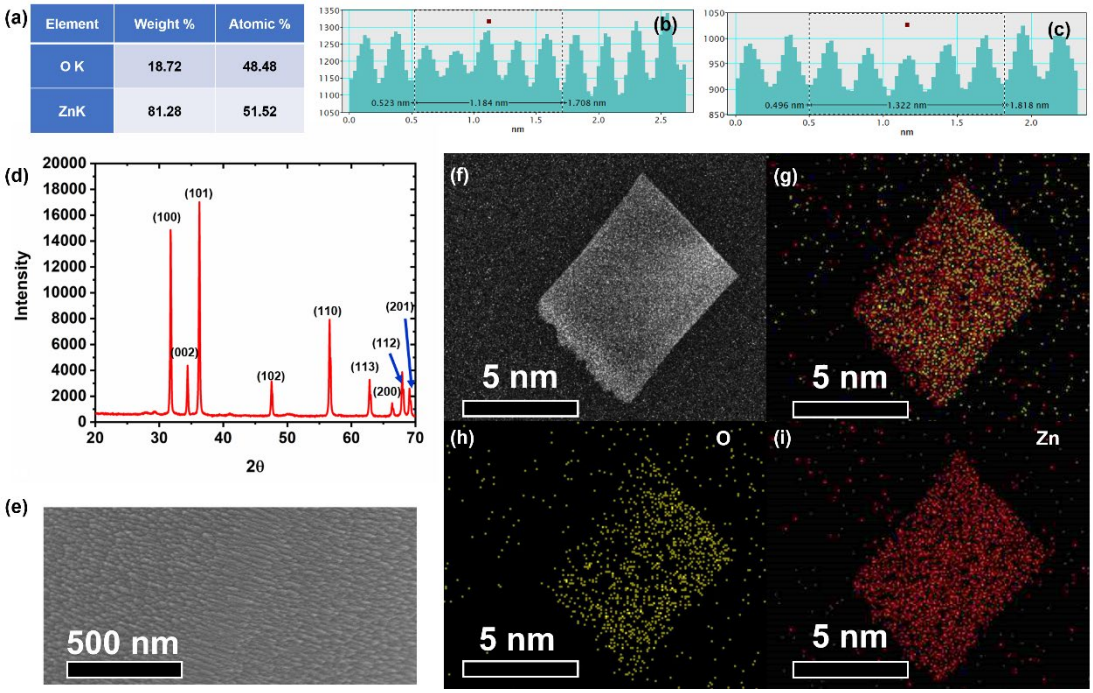

Fig. S1. (a) The mass- and atom-based proportions of Zn and O in the hexagonal ZnO microrods. The interplanar spacings of the (b) Ag NPs and (c) hexagonal ZnO microrods. (d) The XRD pattern acquired from the hexagonal ZnO microrods. (e) A high-resolution SEM image of the Ag NPs/ZnO composite obtained at a magnification of 200,000×. (f) An SEM image of a hexagonal ZnO microrod. (g) An EDS mapping of the same specimen. EDS mappings of the same specimen showing the distribution of (h) O and (i) Zn.

3. The limit of detection (LOD) calculation

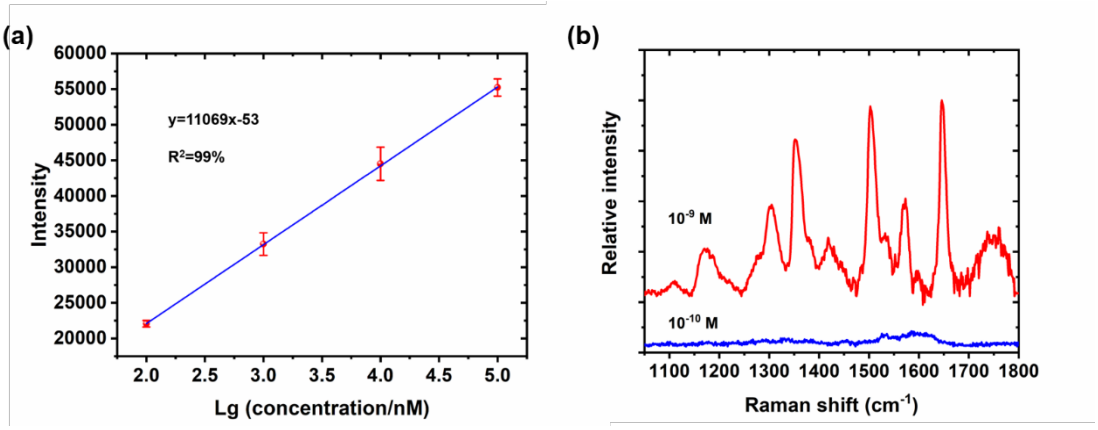

Fig. S2. (a) The SERS intensity at 1360 cm^{-1} obtained using the Ag NPs/ZnO composite as a function of the R6G concentration. (b) The SERS spectra of the Ag NPs/ZnO composite structure substrate with varying concentrations (10^{-9} and 10^{-10} M) of R6G molecules.

The limit of detection (LOD) was defined as the concentration at which the signal-to-noise ratio had a value of 3 and was calculated as 3σ/k, where σ is the standard deviation of replicate blank analysis and k is the slope of the calibration curve. On the basis, the LOD for R6G analysis in the present work was estimated to be approximately 1.03×10^{-9} M. The result is in agreement with the obtained SERS spectra.

4. Enhancement Factor Calculation

The SERS enhancement factor (EF) was calculated as

$$EF = (I_{SERS} / N_{SERS}) / (I_{bulk} / N_{bulk}),$$

where the number of tip molecules is defined as

$$N_{SERS} = A \times N_{sub} \times A_{sub} / \sigma,$$

Here, A is the laser irradiation area (approximately 1.5 μm^2), σ is the area occupied by a single adsorbed R6G molecule (approximately 6.2 nm^2), N_{sub} is the areal population of the Ag NPs (approximately 1.7×10^{-2} nm^{-2}) and A_{sub} is the surface area of the Ag NPs assuming an average diameter of 7 nm. Note that it was assumed here that the Ag NP surfaces were fully saturated with R6G molecules and that one monolayer of these molecules was homogeneously deposited.

The number of tip molecules contributing to the Raman signal in each experiment was

$$N_{bulk} = A \times h \times n_{bulk} = A \times h \times N_A \times \rho_{bulk} / M_{bulk},$$

where h is the laser focusing depth (approximately 10 μm), n_{bulk} is the number of tip molecules per unit volume, ρ_{bulk} is the bulk density (approximately 1.26 g/cm^3), M_{bulk} is the molecular weight of R6G (479.01 g/mol) and N_A is Avogadro's constant (6.02×10^{23}). Using the I_{SERS} and I_{bulk} values determined for the 1360 cm^{-1} band in the SERS spectra, the EF associated with the Ag NPs/ZnO composite was calculated to be approximately 0.9×10^6.

5. In-situ temperature-dependent SERS characterization

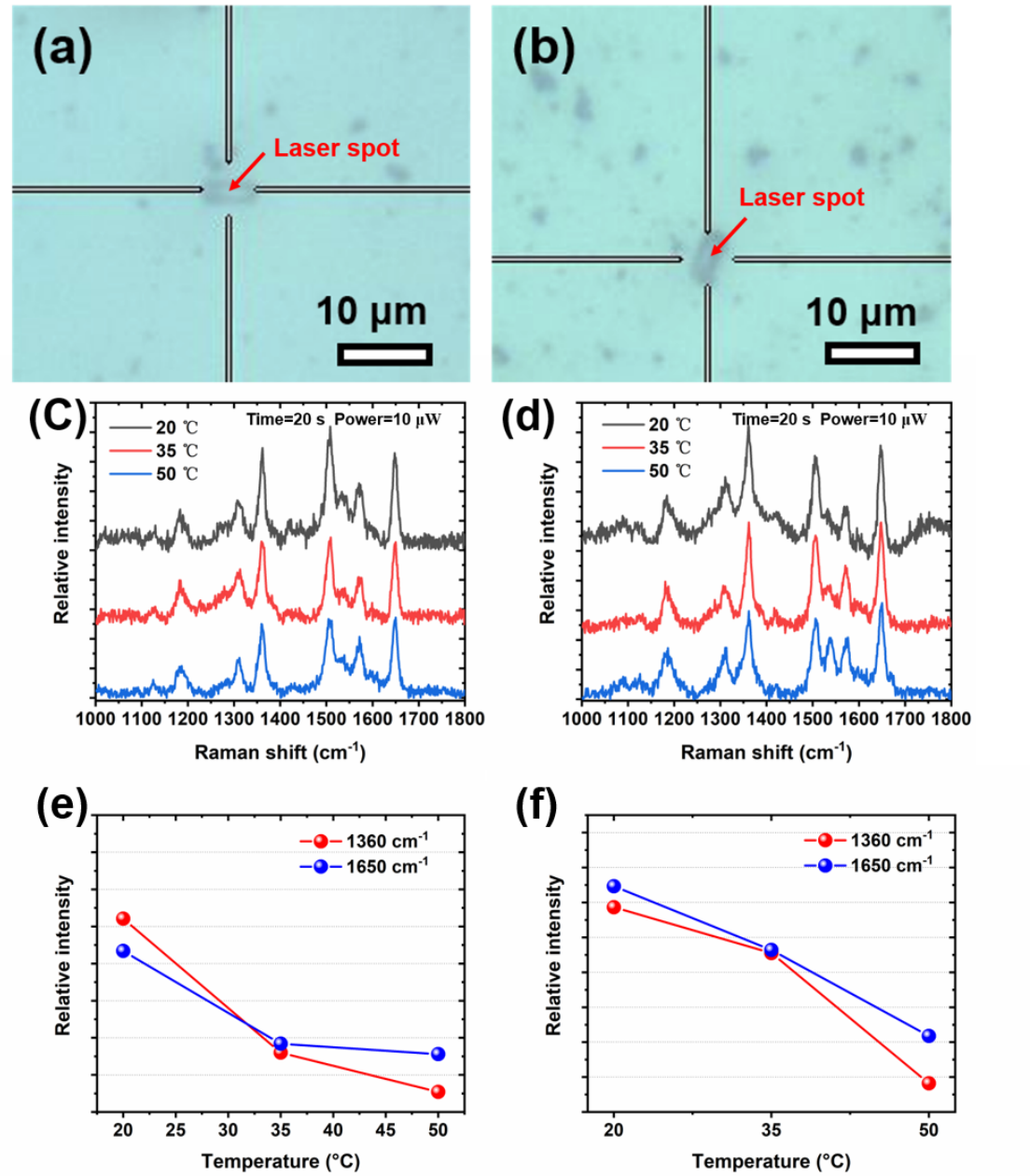

Fig. S3. (a, b) Optical bright-field microscopy images of the Ag NPs/ZnO composite acquired at two points. (c, d) In-situ SERS spectra obtained from the same locations as were used to generate the spectra in (a) and (b), respectively. (e, f) The intensities of the peaks at 1360 and 1650 cm^{-1} in the SERS spectra in (c) and (d), respectively, as functions of temperature.

Optical microscopy images of Ag NPs on the hexagonal ZnO microrod substrate are

presented in Figs. S3a and b. To achieve stable spectral signals during temperature-dependent plasmon-induced catalysis, the SERS spectra were measured after maintaining them at a specific temperature for 60 minutes. Initially, the samples were characterized using SERS spectra at the position marked with red in Figs. S3a and b, after being maintained at a temperature of 20 ˚C for 60 minutes. Subsequently, the ambient temperature was raised to 35 ˚C and maintained for 60 minutes, after which SERS signals were detected at the same position. Finally, the temperature was further increased to 50 ˚C and sustained for 60 minutes, while SERS signal detection was performed at the same position. The corresponding temperature-dependent SERS spectra are displayed in Figs. S3c and d, and the intensities of the 1360 cm^{-1} peaks in these spectra are plotted as functions of temperature in Figs. S3e and f. These results indicate a decrease in peak intensity with an increase in temperature for the in-situ plasmon-induced catalysis process. It is apparent that plasmon-induced catalysis performance is significantly affected, which is illustrated with the intensities of peaks in the SERS spectra. Furthermore, in conjunction with in-situ experiments, it is illustrated that as the temperature increases, the catalytic degradation, which was already close to its limit, can be further enhanced with temperature increasing. This observation demonstrates the changes in the plasmon-induced catalytic properties with temperature during the in-situ SERS process, which have been depicted by the peak intensities of SERS spectra.

6. SERS spectrum of ZnO microrods with R6G molecules

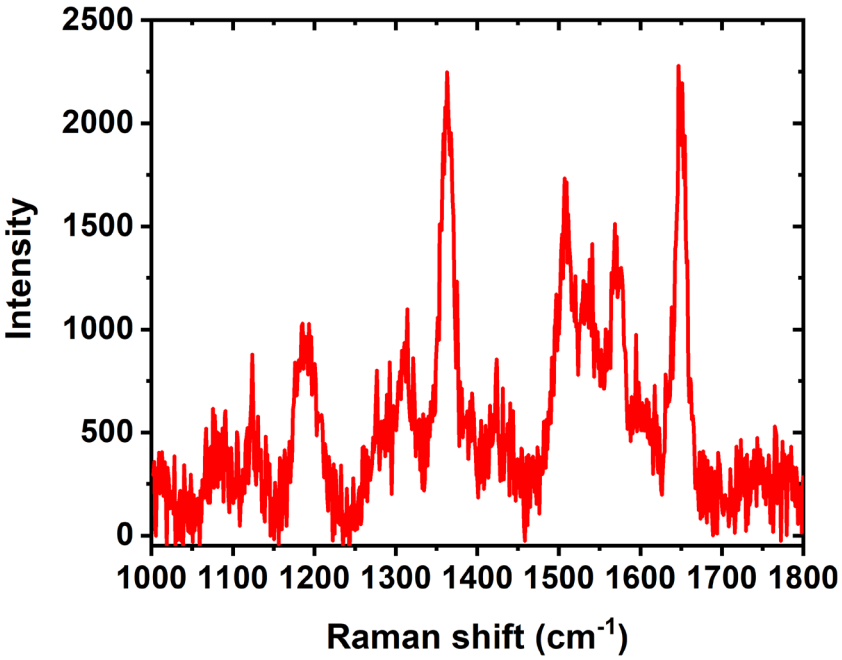

Fig. S4. The SERS spectrum obtained from hexagonal ZnO microrods in the presence of an R6G concentration of 10^{-3} M.

The SERS spectrum in Fig. S4 shows a prominent peak at 1360 cm^{-1} generated by the hexagonal ZnO microrod substrate in conjunction with an R6G molecules concentration of 10^{-3} M, with an intensity of approximately 2300. Note that the SERS characteristics of the same Ag NPs used in the present study were reported in a previous publication (intensity ~1000) by the authors [1]. The results obtained from this research demonstrate an increase in the SERS signal, with an intensity of approximately 80,000 for the Ag NPs/ZnO composite, based on the synergistic effect obtained from combining the Ag NPs and the ZnO substrate.

7. The electron density of states (DOS) calculation details

Slab models of three layers of ZnO (002), two layers of Ag (111) and the junctions between these layers were constructed for simulations. A vacuum spacing of ~15 Å was adopted to avoid the interaction between the periodic images. Molecular dynamics (MD) simulations were performed to simulate the structures of Ag/ZnO junctions at different temperatures based on the universal force field technique [2] in the Forcite module implemented in the Materials Studio software package. A time step of 1.0 fs was employed for the integration together with a total simulation time of 20 ps. During these MD simulations, a canonical (NVT) ensemble and the Nose/Hoover thermostat were used to control the temperature of the system. The electronic properties of the Ag/ZnO junctions were further studied based on first-principles calculations using the Vienna ab initio simulation package (VASP) [3]. The Perdew-Burke-Ernzerhof (PBE) functional [4] based on the spin-polarized generalized gradient approximation (GGA) and PAW pseudopotential [5, 6] was used to account for exchange-correlation interactions associated with ion-electron interactions. A kinetic energy cut-off of 400 eV was adopted and a Monkhorst-Pack k-point grid with a spacing of 0.03 $Å^{-1}$ was used to sample the first Brillouin zone. The valence electron configurations for O, Zn and Ag in these calculations were $2s^2 2p^4$, $3d^{10} 4s^2$ and $4d^{10} 5s^1$, respectively. The experimental band gap of ZnO was reproduced by applying on-site coulomb interactions of U = 10 and 7 eV to Zn 3d and O 2p orbitals, respectively [7]. During the calculations, force and total energy convergence criteria of 0.02 eV/Å and 10^{-4} eV were used.

8. Time-dependent SERS spectra recorded on the Ag NPs/ZnO composite

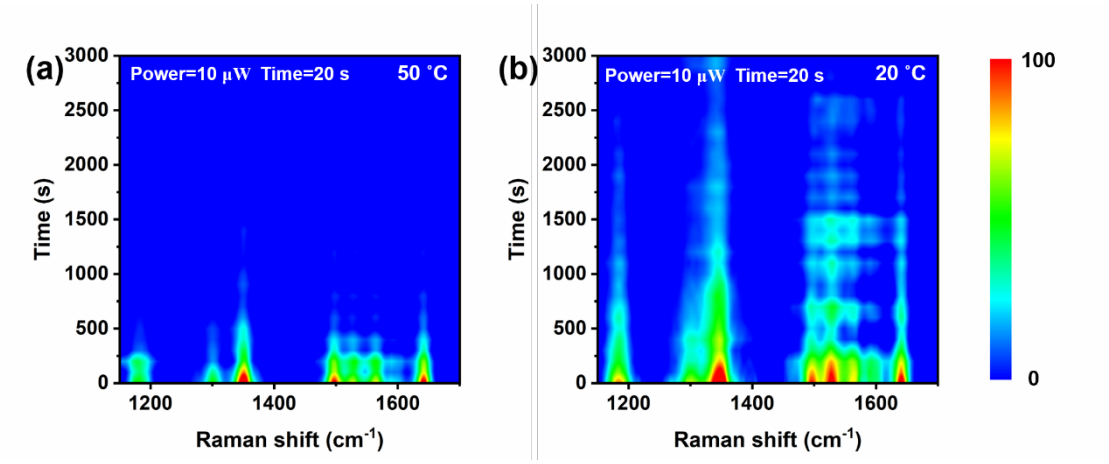

Fig. S5. Time-dependent SERS mapping of R6G molecules on the Ag NPs/ZnO composite substrate at (a) 50 °C and (b) 20 °C.

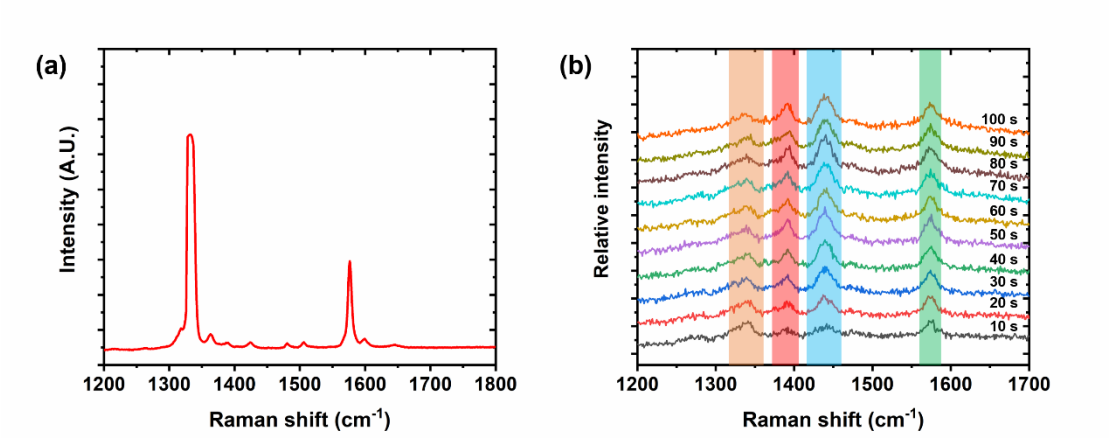

Fig. S6. (a) The Raman spectra of 4-NBT bulk. (b)Time-dependent SERS spectra obtained from the Ag NPs/ZnO composite with adsorbed 4-NBT over time (integration time = 10 s, laser power = 10 μW).

Fig. S6 presents SERS spectra acquired during the intermediate stages of the catalytic reaction on the Ag NPs/ZnO composite. The peak at 1335 cm^{-1} is attributed to the NO_2 stretching vibration associated with the 4-NBT, whereas that at 1575 cm^{-1} corresponds to the C-C stretching vibration, which is shown in Fig. S6a. The peaks at approximately 1390 and 1435 cm^{-1} correspond to the N=N stretching vibrations of DMAB

molecules, as shown in Fig. S6b. These observations highlight the exceptional plasmonic catalytic performance of the Ag NPs/ZnO composite. This material efficiently catalyzed the conversion of 4-NBT to DMAB under extremely weak laser irradiation (10 μW) within a short time span (10 s). When exposed to a more common laser power (100 μW), the 4-NBT underwent direct conversion to DMAB within an extremely short time. However, because of the minimum time setting of 10 s associated with the Raman spectrometer used in this work, direct conversion at this higher power setting could not be assessed.

9. Other supporting data

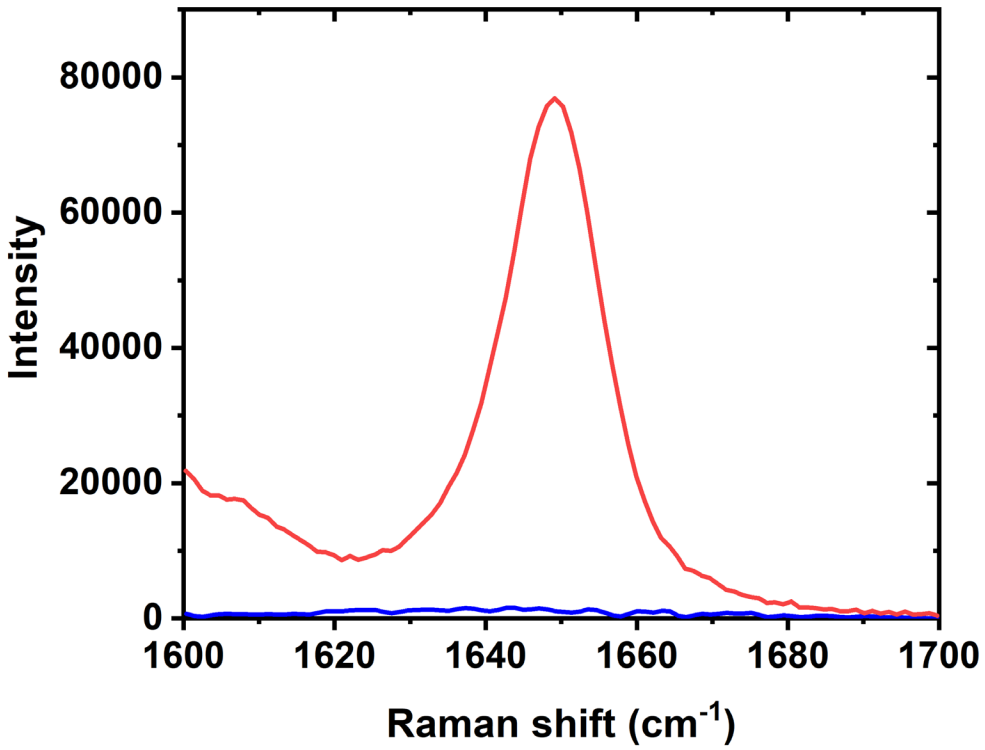

Fig. S7. The SERS spectra peak at 1650 cm^{-1} for Ag NPs/ZnO film (blue line) and Ag NPs/ZnO microrods (red line).

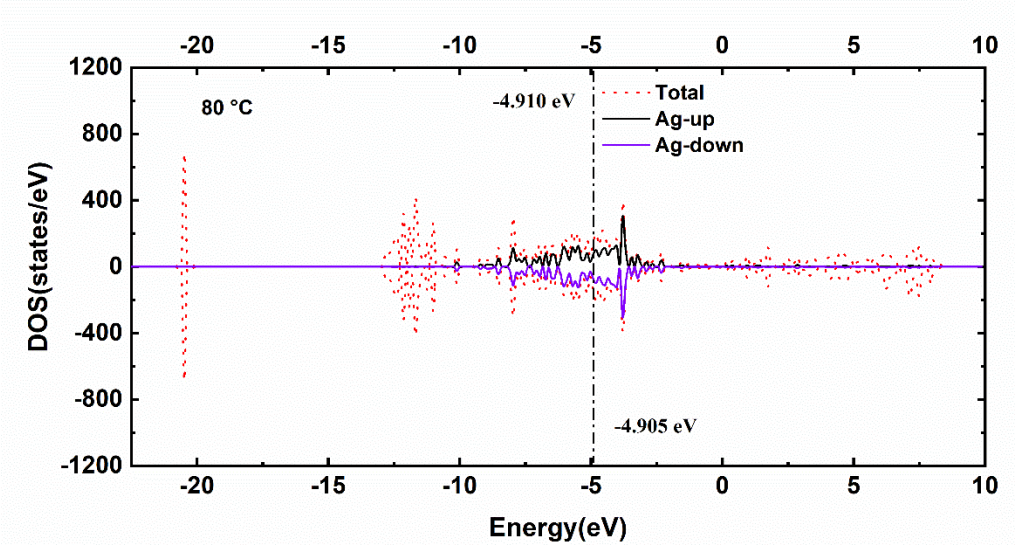

Fig. S8. The DOS data for the Ag-ZnO interface at 80 °C.

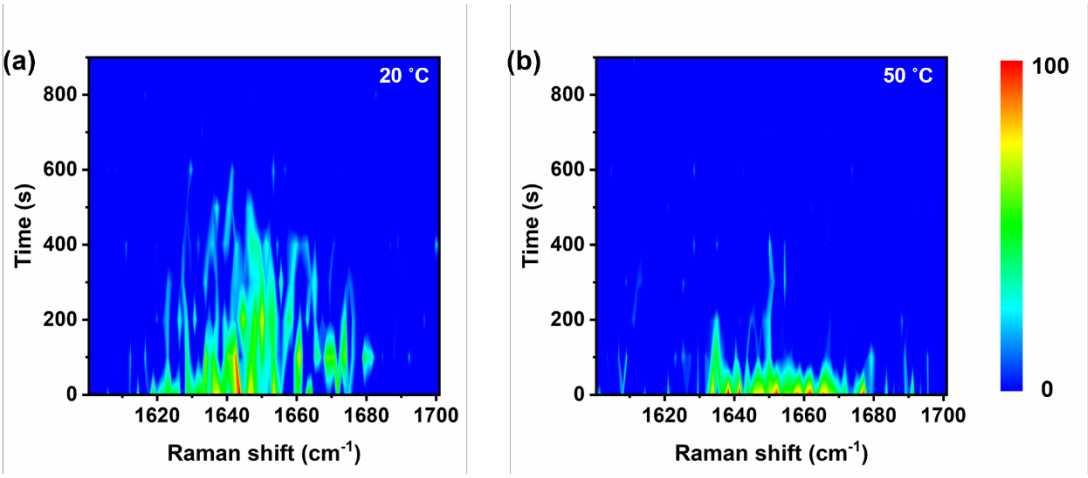

Fig. S9. The temperature-dependent SERS-mapping at the peak of 1650 cm^{-1} with Ag NPs/ZnO film as SERS-active substrate at 20 ˚C (a) and 50 ˚C (b), respectively.

References

S1. Y. Wang, Z. Xiao, X. Feng, S. Shi, D. Liu, R. Li, F. Jiang and J. Liu, *Sensors and Actuators B: Chemical*, 2024, **405**, 135343.

S2. A. K. Rappe, C. J. Casewit, K. S. Colwell, W. A. Goddard and W. M. Skiff, *Journal of the American Chemical Society*, 1992, **114**, 10024-10035.

S3. G. Kresse and J. Furthmüller, *Computational Materials Science*, 1996, **6**, 15-50.

S4. J. P. Perdew, K. Burke and M. Ernzerhof, *Physical Review Letters*, 1996, **77**, 3865-3868.

S5. P. E. Blöchl, *Physical Review B*, 1994, **50**, 17953-17979.

S6. G. Kresse and D. Joubert, *Physical Review B*, 1999, **59**, 1758-1775.

S7. V. N. Jafarova and G. S. Orudzhev, *Solid State Communications*, 2021, **325**, 114166.